Seismic performance and optimal design of framed underground structures with lead-rubber bearings

Zhi-Yi Chen[*1,2], Hu Zhao[2a] and Meng-Lin Lou[1b]

[1]*State Key Laboratory of Disaster Reduction in Civil Engineering, Tongji University,*
1239 Siping Road, Shanghai, China
[2]*Department of Geotechnical Engineering, Tongji University, 1239 Siping Road, Shanghai, China*

Abstract. Lead-rubber bearings (LRBs) have been used worldwide in seismic design of buildings and bridges owing to their stable mechanical properties and good isolation effect. We have investigated the effectiveness of LRBs in framed underground structures on controlling structural seismic responses. Nonlinear dynamic time history analyses were carried out on the well-documented Daikai Station, which collapsed during the 1995 Hyogoken-Nanbu earthquake. Influences of strength ratio (ratio of yield strength of LRBs to yield strength of central column) and shear modulus of rubber on structural seismic responses were studied. As a displacement-based passive energy dissipation device, LRBs reduce dynamic internal forces of framed underground structures and improve their seismic performance. An optimal range of strength ratios was proposed for the case presented. Within this range, LRBs can dissipate maximum input earthquake energy. The maximum shear and moment of the central column can achieve more than 50% reduction, whereas the maximum shear displacement of LRBs is acceptable.

Keywords: lead-rubber bearing; framed underground structure; seismic response; strength ratio; rubber shear modulus; optimal range

1. Introduction

Since they were invented in 1977 by W.H. Robinson (Kelly *et al.* 2006), lead-rubber bearings (LRBs) have been applied worldwide in the seismic design of buildings and bridges as isolation devices, such as in the Hairini Bridge in New Zealand, the Trans-Tokyo bridge in Japan (Kelly *et al.* 2006), the San Francisco City Hall in America (Naeim and Kelly 1999) and the Jiangsu International Financial Center in China. Their isolation effect has been verified numerically (Providakis 2008, Hu 2015) and in actual earthquakes (Asher *et al.* 1997, Nagarajaiah and Sun 2000). To achieve better performance when LRBs are subjected to earthquakes, some researchers have aimed to improve the LRB design. They proposed key design parameters that can be classified into two categories: 1) yield ratio, which is the ratio of LRB yield strength to

---

∗Corresponding author, Associate Professor, E-mail: zhiyichen@tongji.edu.cn

[a]Master Student, E-mail:1432305@tongji.edu.cn

[b]Professor, E-mail: lml@tongji.edu.cn

superstructure weight and 2) isolation period (frequency). Both reflect the relationship between LRB characteristics and superstructure mass. For example, Park and Otsuka (1999) determined the optimal yield ratio of bilinear isolators by studying 1044 two-degree-of-freedom-isolated bridge models and indicated that the ratio of energy absorbed by the isolators to total input energy is related directly to structural responses. It is thus a reliable factor to evaluate the optimal yield ratio. Jangid (2007) investigated the analytical seismic response of multi-story buildings isolated by LRBs under near-fault motion and implied that the optimal yield ratio, for which the criteria is the minimization of top floor absolute acceleration and LRB displacement, ranges from 10-15%. Jangid (2010) pointed out that the optimum yield ratio decreases with increase in isolation period of the structure. Li *et al.* (2013) investigated the seismic response characteristics and optimal parameters of large-scale LRB base-isolated storage tanks at different sites and indicated that the isolation frequency is the primary parameter that affects their isolation effect.

In contrast, a traditional countermeasure is still adopted commonly in the seismic design of underground structures to improve structural seismic performance by enlarging member sections or increasing reinforcement consumption. This method is uneconomical because of the increase in material consumption. It is also unreasonable since this approach may enlarge seismic forces, such as inertia forces (Chopra 2007). Because of the excellent performance of LRBs in superstructures, their introduction into underground structures seems to be a promising way to mitigate seismic damage in underground structures.

However, significant differences exist in seismic design concepts between super- and underground structures. The differences are reflected especially in the following two aspects. 1) Vibration characteristics. Superstructure vibration characteristics are controlled by inertial force. For underground structures, which are confined by surrounding soils, vibration is controlled mainly by soil deformation (Hashash *et al.* 2001). 2) Design structural parameters. In seismic design principles, superstructures are generally designed to have strong columns and weak beams. The philosophy of "strong beams and weak columns" is used mainly in underground structures because of the larger design stiffness of upper plates and beams to resist overburden.

The mechanism of LRBs is quite distinct in reducing seismic responses between super- and underground structures. In superstructures, LRBs are used as a kind of isolation device and many LRBs constitute an isolation layer between the foundation and the superstructure (or between two floors). The natural period of the superstructure is shifted away from the dominant period of earthquake ground motion owing to the isolation layer, and the input earthquake energy is dissipated through yielding of lead cores when subjected to severe earthquakes. Thus the transmitted acceleration into the superstructure is reduced. However, in underground structures, LRBs should no longer be regarded as isolation devices. According to An *et al.* (1997) and Huo *et al.* (2005), central columns are the weak part of underground structures. Fitting LRBs at the bottom end of central columns cannot separate the upper structural components from the bottom plate because lateral walls are still continuous. Additionally, the entire structure is surrounded by soil, so LRBs cannot isolate underground structures from input ground motion. In this circumstance, LRBs behave more like passive energy dissipation devices when subjected to earthquakes according to the classification proposed by Soong and Spencer (2002). They may reduce structural seismic responses in the following ways: 1) installing LRBs at the bottom end of central columns can reduce their stiffness and decrease seismic forces imposed on them; 2) lead cores of LRBs yield and dissipate a large amount of input earthquake energy induced in underground structures through plastic deformation. Damage of the main structure may thereby be alleviated and even avoided.
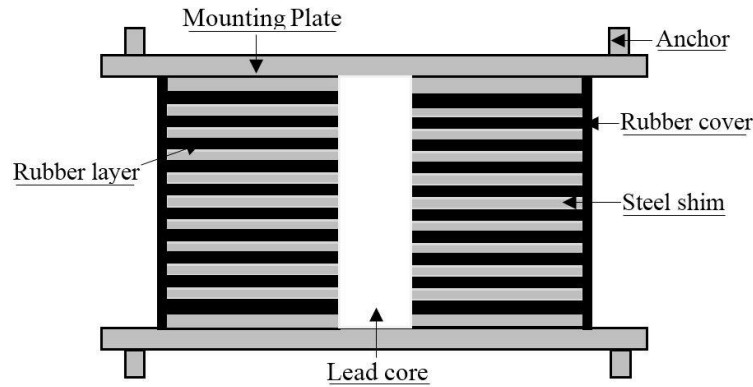
Fig. 1 Sketch of a typical LRB

Based on the above analyses, the research results of LRBs in superstructures, such as the effectiveness and key design parameters and their optimal range, cannot be extrapolated directly to underground structures. Further research is therefore necessary. In this paper, the effectiveness of LRBs in framed underground structures is discussed by performing nonlinear dynamic time history analyses based on the Daikai subway station model. Because of the mechanism of LRBs in framed underground structures, strength ratio, which is the ratio of yield strength of LRBs to yield strength of the central column, is proposed as the key design parameter. The influence of strength ratio on seismic responses of framed underground structures and LRBs is investigated. Moreover, the impact of shear modulus of rubber on the effectiveness of LRBs is studied. Finally, the optimal range of strength ratio is given for the presented case.

2. Brief introduction to LRBs

2.1 Components of LRBs

As shown in Fig. 1, LRBs are composed mainly of a lead core (or more), alternating layers of vulcanized rubber and steel shims, rubber cover, mounting plates and anchors. The lead core provides the initial stiffness of LRBs to minor earthquakes and an additional means of energy dissipation by its plastic deformation when subjected to severe earthquakes. The rubber layers provide horizontal flexibility together with a recentering force. The steel shims increase the vertical stiffness and reduce the lateral bulging of LRBs, which results in a more stable support for the upper structure.

2.2 Analytical models of LRBs

In general, analytical LRB models can be divided into two categories: equivalent linear and nonlinear models. The former, which use approximate linear models to describe actual nonlinear force-deformation behavior, can simplify the analysis of structural response and reduce the required computational time (Hwang and Chiou 1996, Zordan *et al.* 2014). However, their accuracy is relatively low (Matsagar and Jangid 2004). Several types of nonlinear models exist,
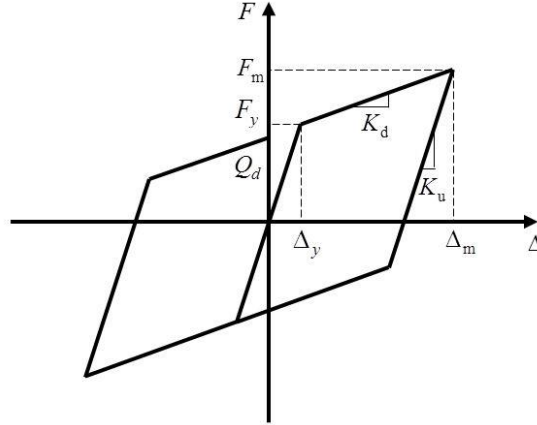
Fig. 2 Bilinear model of LRBs

such as the bilinear model, nonlinear model including axial-load effects (Ryan *et al.* 2005) and the simplified rheology model (Bhuiyan *et al.* 2009). Among them, the bilinear model has been used by many researchers (Mkrtychev *et al.* 2014, Providakis 2008, Hu 2015) owing to its simplicity and acceptable accuracy. Therefore, the bilinear model, as shown in Fig. 2, is used in this study. The main parameters of the bilinear model are its characteristic strength Q_d, post-elastic stiffness K_d and initial stiffness K_u, which can be calculated as follows (Kelly *et al.* 2006, Islam *et al.* 2013)

$$Q_d = \sigma_y A_{pl} , \tag{1}$$

$$K_d = \frac{GA_r}{T_r} , \tag{2}$$

$$K_u = 6.5 K_d (1 + \frac{12 A_{pl}}{A_r}) , \tag{3}$$

where σ_y, A_{pl}, G, A_r and T_r represent the lead yield strength, lead core area, rubber shear modulus, reduced rubber area and total rubber thickness, respectively.

3. Effectiveness of LRBs in framed underground structures

3.1 Analytical model

3.1.1 Background

The Daikai Station is a typical single-story double-span framed underground structure, which was built between 1962 and 1964 by cut-and-cover. It has the general feature of framed underground structures. Namely, the stiffness of plates and lateral walls are commonly designed very large to resist high soil weight and pressure. As a result, central columns seem to be weak parts during an earthquake. In fact, during the Mw 6.9 Hyogoken-Nanbu earthquake, more than 30 columns of the central section of the station collapsed over 110 m. This caused the overlying
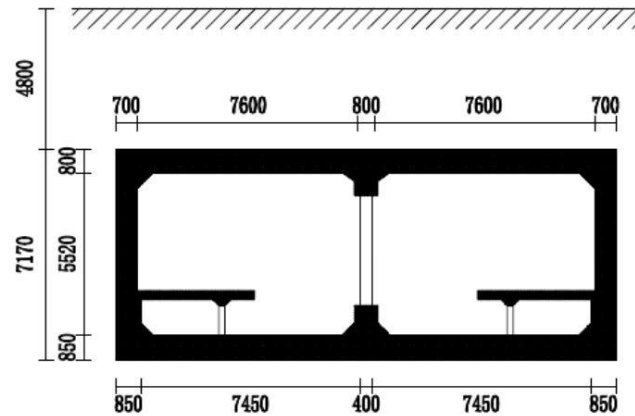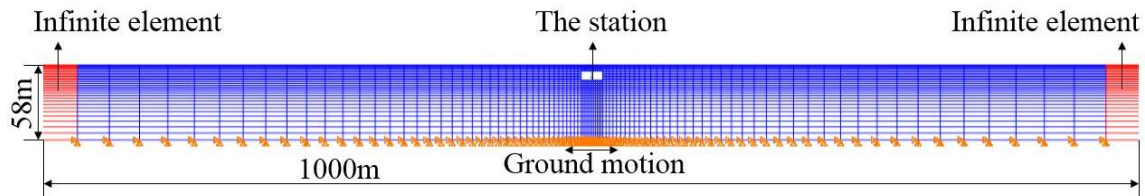
Fig. 3 Cross section of Daikai Station (mm)

Fig. 4 Numerical model of Daikai Station with surrounding soils

concrete roof slab to fail and resulted in a 2.5 m subsidence on national road No. 28, which runs above the subway. The cross section of the destruction area is shown in Fig. 3 (Huo *et al.* 2005).

In addition, the Daikai Station is the first well-documented framed underground structure that collapsed during an earthquake and it received great attention at that time. A number of investigations have been carried out to clarify the failure mechanism of the Daikai Station. Obviously, using the Daikai Station as a case study can benefit the readers to understand the effectiveness and mechanism of LRBs in framed underground structures. Therefore, the Daikai Station model was used as an analytical model to evaluate the effectiveness of LRBs in framed underground structures.

3.1.2 Modeling of the station with surrounding soils

All numerical models were developed using commercial software package ABAQUS (2011). Because the configuration and dimensions of the cross section are the same along the axis of the station and the dimension in the longitudinal direction is greater than in the other two directions, a two-dimensional plane strain model that is 1000 m long and 58 m high is used, as shown in Fig. 4. To decrease the impact caused by seismic reflection, infinite elements are imposed on the lateral boundaries. A free boundary condition is imposed on the top boundary. The bottom boundary, on which horizontal and vertical displacements are fixed, is placed 58 m from the surface. It corresponds to the top of the gravel layer in Port Island. All boundaries are assumed to be waterproof.

The constitutive soil model is simulated by the Mohr-Coulomb model. According to the destruction area, soil parameters in D-1 and B-3 boreholes are taken as the basis of model soil

Table 1 Soil parameters of Daikai Station

Name	Depth (m)	Unit weight (kN/m³)	Cohesion yield stress (kPa)	Friction angle (°)	Young's modulus (MPa)	Poisson's ratio
Fill	0-1	19	20	15	101.308	0.33
Holocene clay	1-2	19	30	20	100.320	0.32
Holocene sand	2-4.8	19	1	40	147.840	0.32
Pleistocene sand	4.8-8	19	1	40	195.972	0.40
Pleistocene clay	8-17	19	30	20	290.342	0.30
Pleistocene gravel	17-	20	1	40	560.045	0.26

(Cao *et al.* 2002). Soil layers and parameters for modeling are summarized in Table 1. Because of the lack of data, cohesion and friction angles of each stratum are chosen as follows: man-made fill, 20 kPa, 15°; clay, 30 kPa, 20° and sand and gravel, 1 kPa, 40° (Das 2008).

The structure without central column is assumed to exhibit elastic behavior throughout the analysis. The concrete in the structure is modeled as a linear elastic material, with unit weight 25 kN/m³, Poisson's ratio 0.15 and Young's modulus 24 GPa for the frame, and 7 GPa for the column. The actual column spacing is taken into consideration with the reduced stiffness. The interface between the structure and the ground is modeled as a frictional surface. The contact can open if there is a tensile normal stress or it can slip if the magnitude of the applied shear stress is larger than the shear strength, which is assumed to follow the Coulomb friction law. A coefficient of friction, μ, equal to 0.4 is assumed, which corresponds to a friction angle of 22°. No cohesion between the structure and ground is included (Huo *et al.* 2005).

2952 plain strain elements (CPE4R) are used to simulate the soil. 91 beam elements (B21) are used to simulate the structure. As shown in Fig. 4, the grid closed to the structure is refined and a single bias with the value of 5.0 is defined to change the mesh density from the structure to the lateral boundary.

3.1.3 Modeling of LRBs

The central column of Daikai Station is ~5 m high with a rectangular cross section of 0.4 m by 1.0 m. Referring to the design procedure for LRBs in buildings and bridges (Kelly *et al.* 2006, Naeim and Kelly 1999), two square 0.4 m×0.4 m LRBs are set at the bottom end of the central column. In this section, the rubber shear modulus, lead diameter, rubber layer thickness, number of rubber layers and steel shim thickness are 0.4 MPa, 0.1 m, 4 mm, 10 and 3 mm, respectively. According to Eqs. (1)-(3), the characteristic strength Q_d, post-yield stiffness K_d and initial stiffness K_u for each LRB are 66.8 kN, 936.5 kN/m and 12213.1 kN/m, respectively. The cross section of Daikai Station with LRBs is shown in Fig. 5. These two LRBs are parallel to each other and are in series with the central column. The total characteristic strength Q_d, post-yield stiffness K_d and initial stiffness K_u for the two LRBs are 133.6 kN, 1873.0 kN/m and 24426.2 kN/m, respectively. The entire part, which is composed of the two LRBs and the central column, is parallel to the lateral walls to resist horizontal earthquakes.

One horizontal spring and one vertical spring are used to simulate LRB. The horizontal spring is used to simulate the bilinear shear-displacement relationship of LRB under horizontal force. The vertical spring is used to simulate the axial deformation of LRB. It is assumed that the horizontal spring and the vertical spring work independently.
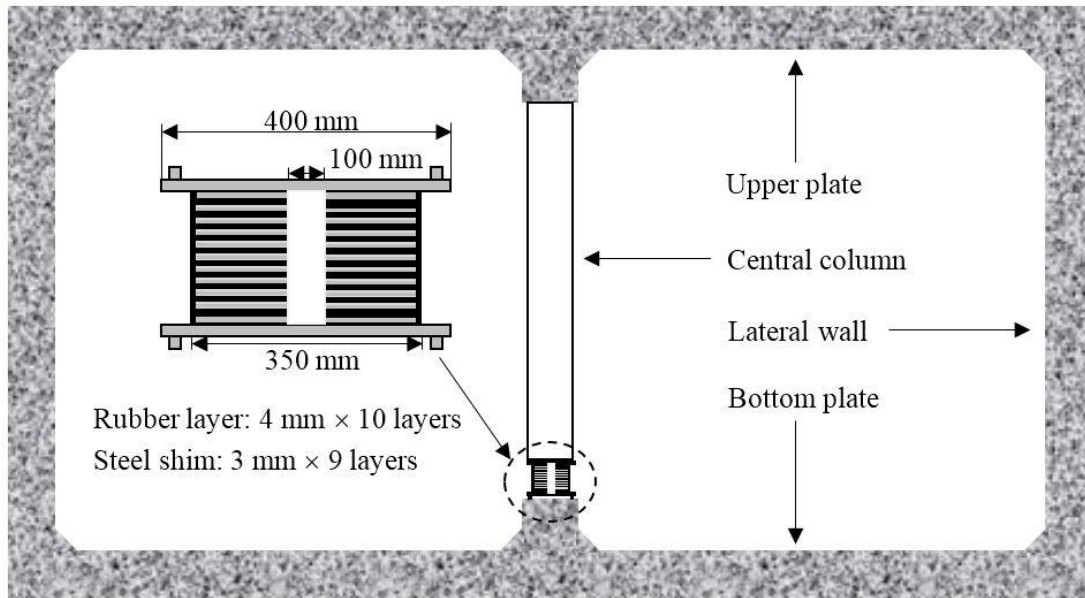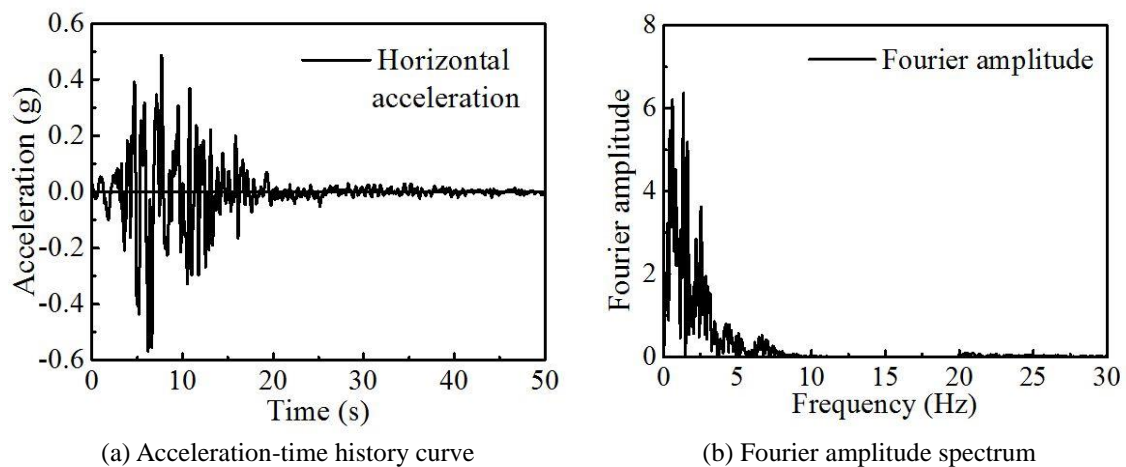
Fig. 5 Cross section of Daikai Station with LRBs

(a) Acceleration-time history curve   (b) Fourier amplitude spectrum

Fig. 6 Input ground motion (horizontal)

3.1.4 Input ground motion

According to Japanese Code (JGS-4001-2004 2006), the artificial bedrock in this paper is set at a depth of 58 m where the shear wave velocity is greater than 300 m/s. A horizontal ground motion and a vertical ground motion are simultaneously imposed at the artificial bedrock for numerical analyses. The horizontal ground motion is recorded at Port Island strong motion station during the Hyogoken-Nanbu earthquake. The vertical ground motion is obtained by adjusting the amplitude of the horizontal acceleration. The values of the maximum horizontal and vertical accelerations are 0.58 and 0.16 g (5.7 and 1.6 m/s^2). The horizontal ground motion is shown in Fig. 6. Because Port Island and Daikai Station are closely located and have similar geological conditions, the ground

motion recorded at Port Island is chosen to make simulated results closer to actual conditions.

3.2 Verification of numerical model and analytical method

Nonlinear dynamic time history analyses are performed to evaluate the effectiveness of LRBs in the Daikai Station. The Full Newton solution technique is chosen for dynamic step in ABAQUS (2011). The processing time is around 30 minutes in a computer with Inter Core i5-4210M. The maximum shear displacement, axial force and shear of the central column without LRBs are 32 mm, 5103 kN and 829 kN, respectively. Compared with the results of Huo *et al.* (2005) and Parra-Montesinos *et al.* (2006), the presented finite element model and analytical method appear accurate and reliable.

3.3 Results analysis

A number of investigations have been carried out to clarify the failure mechanism of Daikai Station. For example, Iida *et al.* (1996) indicated that the inertial force of overburden soils above the structure could be the primary cause of failure. An *et al.* (1997) suggested that the central column failed in shear because of lateral displacements imposed by earthquake-induced ground motion. Huo *et al.* (2005), Parra-Montesinos *et al.* (2006) deemed that the axial force rising in a column caused by the earthquake weakened the shear capacity, and was the reason why the station failed. In view of the above fact, destruction of the central column is the main cause of failure of the station. Therefore, the seismic responses of the central column and LRBs were selected to evaluate the effectiveness of LRBs in framed underground structures.

3.3.1 Seismic responses of central column

Comparisons between seismic responses of the structure with and without LRBs are shown in Fig. 7. The shear displacement-time history curves of the central column with and without LRBs are plotted in Fig. 7(a). They are obtained by subtracting the lateral displacement at the top end of the central column from that at the bottom end of the central column. In the original structure, the peak value was 32 mm. After LRBs were installed, it reaches 43 mm. The increase is small and has little effect on the structure.

Figs. 7(b)-(c) present the shear and moment time history curves of the central column with and without LRBs. It should be noted that, the maximum shear and moment occur at the bottom end of the central column in the structure without LRBs. After LRBs are installed at the bottom end of the central column, the maximum shear and moment occur at the top end of the central column. Obviously, it is rational to focus on the maximum values when we evaluate the effectiveness of LRBs. So, in Figs. 7(b)-(c), the plots without LRBs are drawn according to numerical results of the bottom end of the central column. And the plots with LRBs are drawn according to numerical results of the top end of the central column. From these two figures, it can be found that fitting LRBs to the central column reduces the maximum shear from 829 kN to 205 kN, which means a 75% reduction. The maximum moment of the central column falls from 1721 kN·m to 542 kN·m, namely a 69% reduction.

Based on the dimensions of the central column and parameters of the concrete and reinforcements (Parra-Montesinos *et al.* 2006, Yamato *et al.* 1996), the thrust-moment bearing capacity curve of the central column is plotted in Fig. 7(d). This figure also presents the thrust-moment relationship of the central column with and without LRBs. The plot without LRBs

(a) Shear displacement-time histories

(b) Shear-time histories

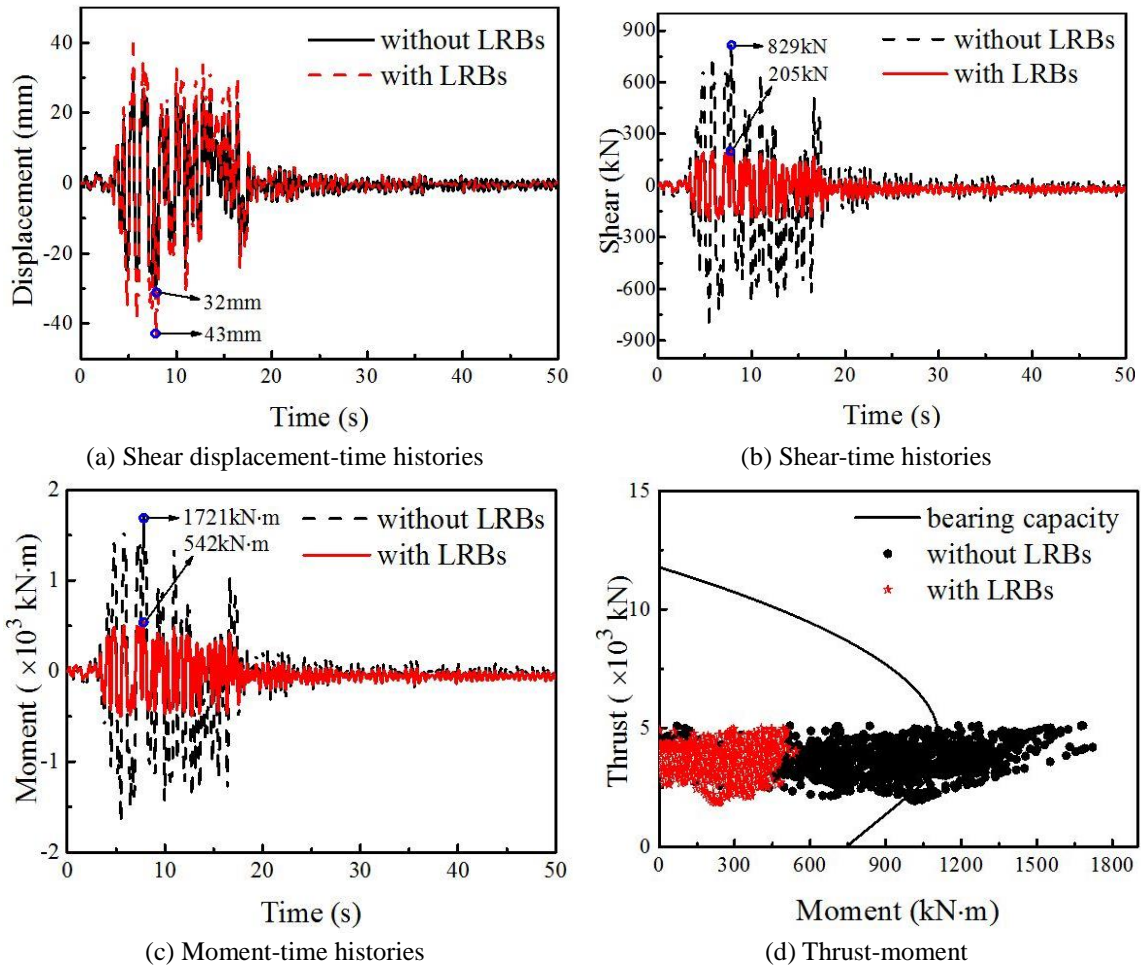(c) Moment-time histories

(d) Thrust-moment

Fig. 7 Comparisons of seismic responses of central column with and without LRBs

is drawn according to numerical results at the bottom end of the central column. And the plot with LRBs is drawn according to numerical results at the top end of the central column. The internal forces of the central column exceed its thrust-moment bearing capacity curve in the original structure, which leads to severe damage of the central column. After LRBs are set, the maximum shear and moment are reduced significantly whereas the maximum thrust shows little change. Consequently, the internal forces of the central column would not exceed its bearing capacity and remain undamaged.

3.3.2 Seismic responses of LRBs

Fig. 8(a) presents the time history curve of the total energy dissipation of the two LRBs. From 5 to 17 s, the LRB energy dissipation increases sharply and coincides with strong shocks (see Fig. 6(a) and 8(a)). When the earthquake weakens, LRBs remain in the elastic stage and no longer dissipate energy. Fig. 8(b) shows the shear displacement-time history curve of LRBs, which is obtained by subtracting the displacement at the top plate of the LRBs from that at the bottom plate.
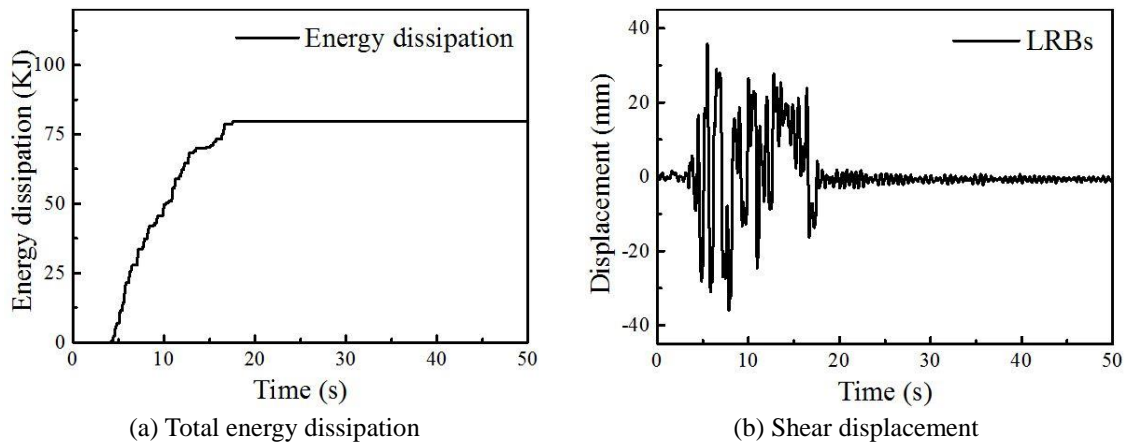
(a) Total energy dissipation   (b) Shear displacement

Fig. 8 Seismic responses of LRBs

The maximum shear displacement of LRBs is 36 mm. The residual shear deformation of LRBs is very small (~0.5 mm), which is beneficial to the replacement or repair of LRBs after earthquakes.

3.3.3 Mechanism of LRBs in framed underground structures

Frequency and Fourier analyses were carried out to explore the mechanism of LRBs in mitigating seismic damage of framed underground structures. The nature period of the structure, the predominant period of the surrounding soils and that of the seismic wave were 0.19 s, 0.53 s and 0.73 s, respectively. Compared with the natural period of the structure, the predominant period of the surrounding soils is relatively close to that of the seismic wave. This phenomenon leads to a relatively large shear deformation of surrounding soils. It also implies that the structure may be mainly affected by shear deformation of surrounding soils rather than vibration itself. LRB installation at the bottom end of the central column in framed underground structures decreases the lateral stiffness of the central column with LRBs. Because a central column with LRBs is parallel with lateral walls to resist horizontal earthquakes, a smaller lateral stiffness of the central column with LRBs results in less distribution of seismic action on the central LRB column. The internal forces of the central column are reduced significantly. As the weak part of framed underground structures when subjected to severe earthquakes, the central column is protected from damage. LRBs dissipate a large amount of input earthquake energy through plastic deformation of lead cores. In addition, the residual shear deformation of LRBs is very small owing to a recentering force that is provided by the rubber layers. This point is very helpful to the replacement or repair of LRBs after earthquakes. In summary, LRBs, as a kind of displacement-based passive energy dissipation device, can improve the seismic performance of framed underground structures effectively for the case presented.

4. Optimal parameter analyses of LRBs

Installing LRBs at the bottom end of the central column cannot isolate the upper structural components from the bottom plate. Consequently, the yield ratio, which is the ratio of LRB yield strength to superstructure mass, has no meaning in underground structures. The isolation period

(frequency) would also be an unsuitable design parameter for LRBs in underground structures because LRBs are no longer used as isolation devices. If we consider the mechanism of LRBs in framed underground structures, the strength ratio, α, is proposed as the optimal design parameter herein. It is defined as

$$\alpha = \frac{F_{y,LRBs}}{F_{y,cc}},\tag{4}$$

where $F_{y,LRBs}$ denotes the total yield strength of the two LRBs fitted at the bottom end of the central column and $F_{y,CC}$ denotes the yield strength of the central column. The influence of strength ratio α and rubber shear modulus G on the effectiveness of LRBs in a framed underground structure is investigated by studying 42 cases.

4.1 Case design

Fig. 9 shows the idealized relationship between LRBs and the central column. It is expected that when subjected to severe earthquakes, LRBs enter the plastic state prior to the main structure to dissipate energy and to suppress amplitudes of vibrations so that the main structure will only be damaged lightly or remain elastic. In Fig. 9(a), the two springs represent LRBs and the central column, respectively. F_y and K represent the lateral yield strength and initial stiffness, respectively. Fig. 9(b) illustrates the bilinear force-displacement model of LRBs and the central column, where F and Δ denote the shear and displacement, respectively. $F_{y,LRBs}$ should be smaller than $F_{y,CC}$.

Forty-two cases were studied numerically to determine the influence of α and G on the effectiveness of LRBs in a framed underground structure. First, three levels of G were used, namely 0.4 MPa, 0.6 MPa and 0.8 MPa. They are commonly used in the practice. Then, fourteen values of α were set at 0.01, 0.05, 0.10, 0.14, 0.18, 0.22, 0.27, 0.32, 0.38, 0.44, 0.51, 0.66, 0.83 and
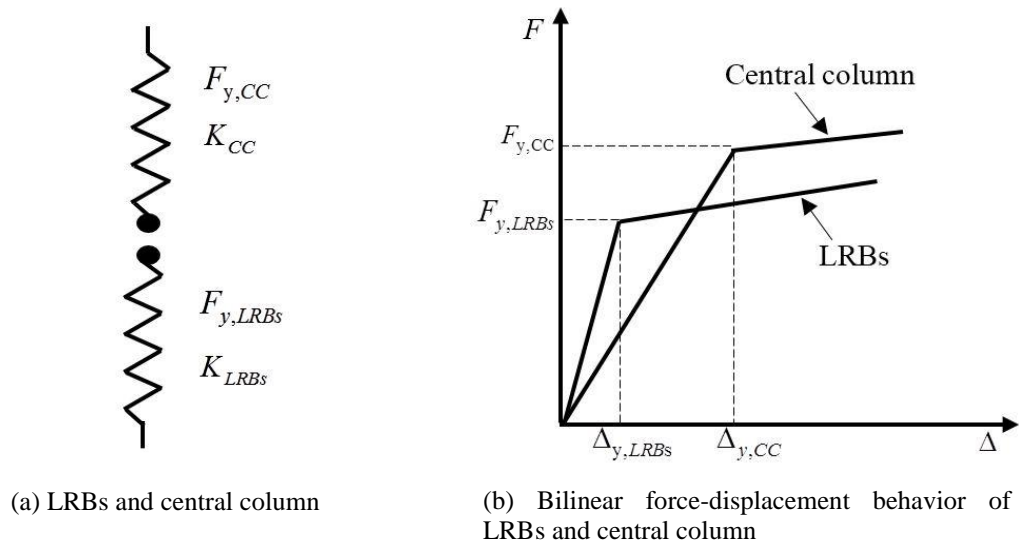

(a) LRBs and central column   (b) Bilinear force-displacement behavior of LRBs and central column

Fig. 9 Idealized relationship between LRBs and central column

(a) Total initial stiffness for two LRBs   (b) Yield displacement of LRBs
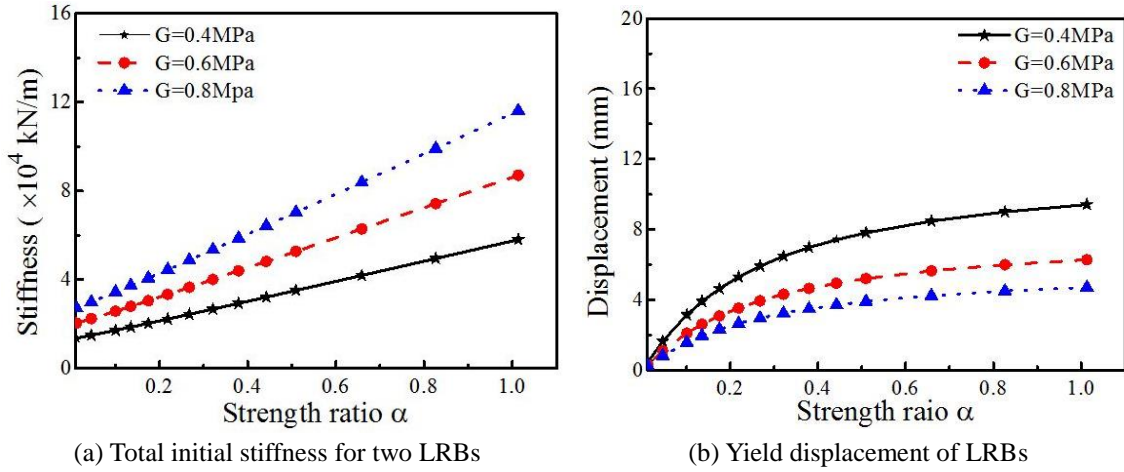
Fig. 10 Total initial stiffness and yield displacement of LRBs

1.01. According to the shear force-displacement curve of the central column in Daikai Station (Parra-Montesinos *et al.* 2006), the yield strength of the central column is ~540 kN. $F_{y,LRBs}$ can be calculated from Eq. (4). The LRB dimensions, rubber layer thickness, number of rubber layers and steel shim thickness are the same as those in section 3. Other parameters needed for the numerical study can be calculated (Kelly *et al.* 2006, Naeim and Kelly 1999).

The total initial stiffness and yield displacement of LRBs calculated for each case are shown in Fig. 10. As shown in Fig. 10(a), the total initial stiffness of LRBs increases almost linearly with increase in α and the rate of increase is faster for larger G. With an increase in G, the total initial stiffness of the LRBs also increases and the influence of G on the total initial stiffness is greater when α is larger. In Fig. 10(b), the yield displacement of LRBs increases with increase in α and decreases with increase in G. All LRB features mentioned herein would affect the effectiveness of LRBs in underground structures, which will be discussed later.

4.2 Results analysis

4.2.1 Effects on shear and moment of central column

Fig. 11 shows the maximum shear and moment of the central column for each case. With an increase in α, the maximum shear and moment of the central column increase almost linearly. This occurs because the total initial LRB stiffness increases with increase in α (see Fig. 10(a)). The lateral stiffness of the central column with LRBs increases with increase in total initial LRB stiffness. This leads to an increased distribution of seismic action on the central column with LRBs, which is parallel to the lateral walls to resist horizontal earthquakes. A greater distribution of seismic action on the central column with LRBs results in a larger shear and moment of the central column. Using the same reason, the maximum shear and moment of the central column increase with increase in G, as shown in Figs. 11(a)-(b).

4.2.2 Effects on shear and shear displacement of LRBs

It is shown in Fig. 12(a) that the maximum shear of LRBs increases with an increase in α or G. This occurs because of the same reason as the maximum shear of the central column discussed
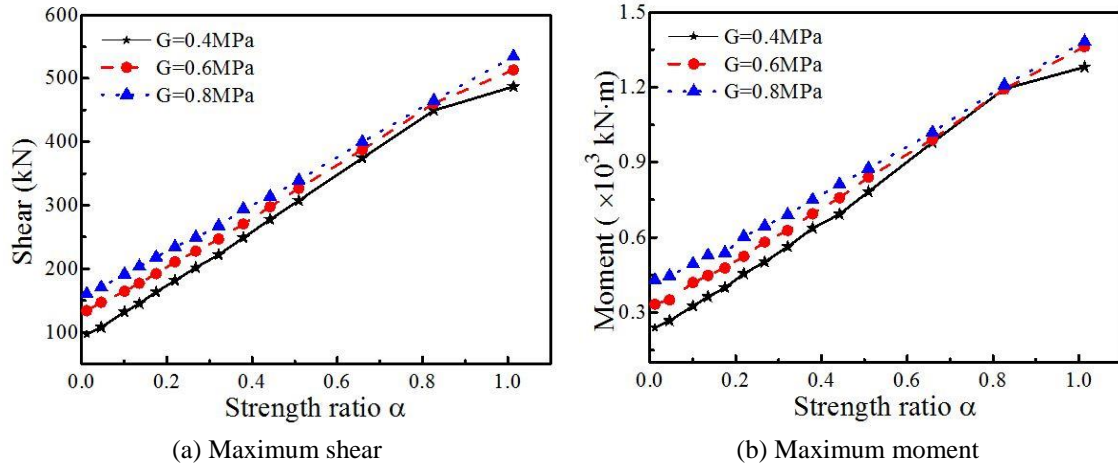
(a) Maximum shear

(b) Maximum moment

Fig. 11 Maximum shear and moment of central column

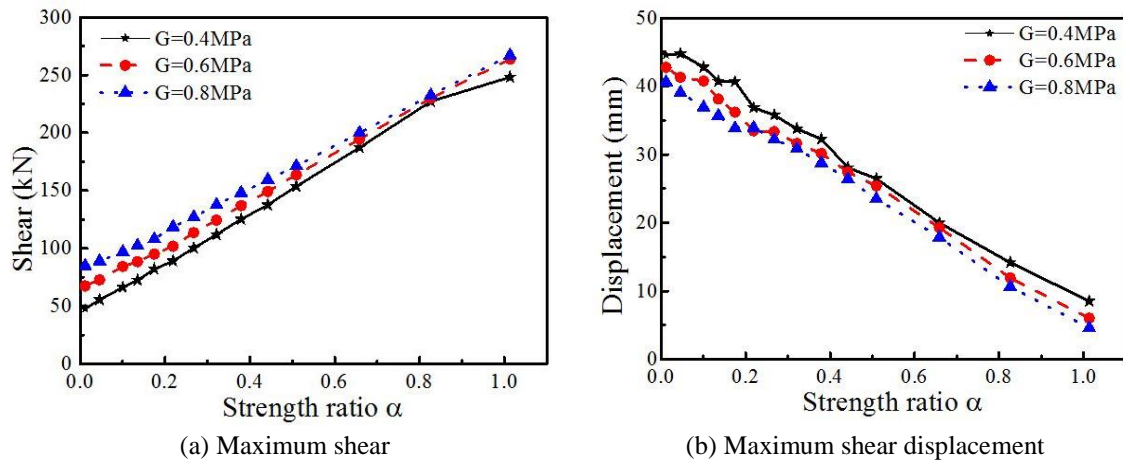

(a) Maximum shear

(b) Maximum shear displacement

Fig. 12 Maximum shear and shear displacement of LRBs

above. Fig. 12(b) illustrates the maximum shear displacement of LRBs. If we compare Fig. 12(b) with Fig. 10(b), it can be seen that the maximum shear displacement of LRBs decreases, whereas the yield displacement of LRBs increases with increase in α. When α reaches 1.01, the shear displacement of LRBs (8.5 mm, 6.0 mm and 4.6 mm, which correspond to G=0.4 MPa, 0.6 MPa and 0.8 MPa, respectively) does not reach their yield displacement (9.4 mm, 6.3 mm and 4.7 mm, which correspond to G=0.4 MPa, 0.6 MPa and 0.8 MPa, respectively). The LRBs therefore remain in an elastic state under the earthquake. This is not the expected case.

Fig. 13 shows typical shear-shear displacement hysteresis curves of LRBs. Only the cases for α=0.05, 0.27, 0.83 and 1.01 at G=0.4 MPa are presented. When α is very small (for example α=0.05), although the shear displacement of LRBs is large, the shear of LRBs is small, which results in a flat hysteresis curve and less energy dissipation. When α is too large (for example α=0.83), although LRBs enter the plastic stage, the plastic deformation is very small, which leads to a narrow hysteresis curve. This means that the energy dissipation capacity of LRBs has not been
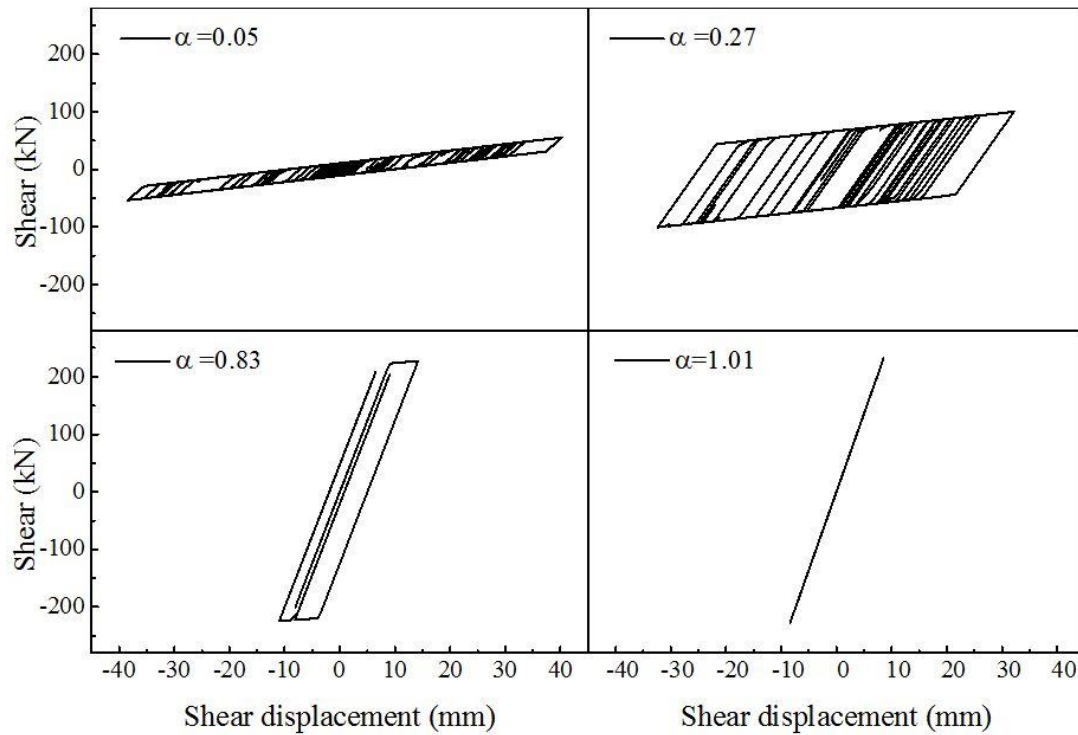
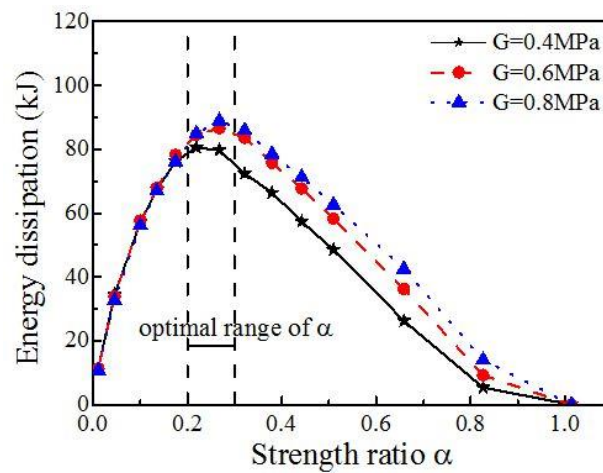Fig. 13 Shear-shear displacement hysteresis curve of LRBs at *G*=0.4 MPa

Fig. 14 Total energy dissipation of LRBs

exerted fully. When α exceeds 1 (for example α=1.01), LRBs would not enter the plastic stage during the entire earthquake and no energy is dissipated by the LRBs. The case in which α is equal to 0.27 is the best for dissipating the input earthquake energy.

In addition to the shear-shear displacement hysteresis curves, the energy dissipation capacity of LRBs can be observed directly from the magnitude of energy dissipated by LRBs, as shown in Fig.

14. With an increase in α, the energy dissipated by LRBs increases first and then decreases. This means that there must be an optimum α at which the energy dissipation of LRBs attains a maximum value. If α is greater than 1, no energy would be dissipated by LRBs. Even when α reaches 1.01, the maximum shear and moment of the central column are reduced compared with the maximum shear and moment of the central column without LRBs (compare Figs. 11(a)-(b) and Figs. 7(b)-(c)). This is because fitting LRBs at the bottom end of the central column still decreases the lateral stiffness of the central column with LRBs to reduce the seismic forces imposed on it in this case.

Fig. 14 also shows the influence of G on energy dissipation of LRBs. When α is smaller than 0.2, it is almost uninfluenced by the change in G. When α exceeds 0.2, the LRBs dissipate more input earthquake energy with increase in G, but the maximum shear and moment of the central column increase simultaneously (see Figs. 11(a)-(b)). The change in G almost has no influence on the optimal α at which the LRBs dissipate the most input earthquake energy.

4.2.3 Optimal range of α

For the case presented, it can be concluded from the above discussions that the maximum shear and moment of the central column is nearly proportional to α, whereas the maximum shear displacement of the LRBs is almost inversely proportional to α. This implies that a compromise should be made between the reduction in internal forces of the central column and that of the shear displacement of LRBs in designing LRBs in framed underground structures. When α is set between 0.2 and 0.3, the maximum shear and moment of the central column can achieve more than a 50% reduction whereas the maximum shear displacement of LRBs is acceptable. Besides, the lead cores can dissipate the most input earthquake energy in this range of α. Therefore, the optimal range of α for the presented structure is suggested to be 0.2-0.3.

In addition, Fig. 14 shows that an appropriate increase in G can improve the energy dissipation capacity of LRBs during an earthquake when α is set in the optimal range. This is helpful to take full advantage of LRBs in the seismic design of framed underground structures.

5. Conclusions

The effectiveness of LRBs in framed underground structures was studied using the Daikai subway station as analytical model. The influence of strength ratio α and rubber shear modulus G on seismic responses of the structure and LRBs were also investigated. The optimal range of α was given for the case presented. Based on the numerical results, the following conclusions can be made:

• LRBs can improve the seismic performance of framed underground structures effectively as a kind of passive energy dissipation device. For the case presented, the internal forces of the central column exceed its thrust-moment bearing capacity curve in the original structure, which leads to severe damage of the central column. After LRBs are set, the maximum shear and moment achieve more than a 50% reduction whereas the maximum thrust shows little change. Consequently, the internal forces of the central column would not exceed its bearing capacity and the safety of the central column can be ensured.

• The effectiveness of LRBs in framed underground structures is achieved because of the following. First, installing LRBs at the bottom end of the central column in framed underground structures decreases the lateral stiffness of the central column with LRBs. Because

the central column with LRBs is parallel to the lateral walls to resist horizontal earthquakes, the smaller lateral stiffness of the central column with LRBs results in less distribution of seismic action on it. The internal central column forces are greatly reduced. Second, LRBs dissipate a large amount of input earthquake energy through plastic deformation of lead cores when subjected to severe earthquakes. Third, the residual shear deformation of LRBs is very small owing to the recentering force provided by rubber layers.

• For the case presented, the seismic responses of the structure and LRBs are very sensitive to the strength ratio α. With an increase in α, the maximum shear and moment of the central moment and the maximum shear of LRBs increase almost linearly whereas the maximum shear displacement of LRBs decreases. With increase in α, the energy dissipated by LRBs increases first and then decreases.

• For the case presented, there exists a certain value of α, at which LRBs can dissipate the most input earthquake energy for a given ground motion. If α exceeds 1, LRBs would not enter the plastic stage and no energy would be dissipated through them. For the structure studied in this paper, the optimal range of α is 0.2-0.3. When α is set in this range, the maximum shear and moment of the central column can achieve more than a 50% reduction whereas the maximum shear displacement of LRBs is acceptable. Moreover, LRBs can dissipate the most input earthquake energy. An appropriate increase in G can improve the energy dissipation capacity of LRBs during an earthquake when α is set in the optimal range.

It should be noted that, due to the overburden, the axial compression ratio of framed underground structures is generally larger than that of superstructures. It will bring a challenge to the vertical bearing capacity of LRBs which may limit the application of LRBs in framed underground structures. In addition, the presented study only verified the effectiveness of LRBs numerically by one case. Therefore, it is preferable to further validate the effectiveness by shaking table texts. The influences of structural styles, input ground motion features and site conditions should be systematically studied in the future.

References

An, X.H., Shawky, A.A. and Maekawa, K. (1997), "The collapse mechanism of a subway station during the Great Hanshin Earthquake", *Cement Concrete Compos.*, **19**(3), 241-257.

Asher, J.W., Hoskere, S.N., Ewing, R.D., Mayes, R.L., Button, M.R. and Van Volkinburg, D.R. (1997), "Performance of seismically isolated structures in the 1994 Northridge and 1995 Kobe earthquakes", *Proceedings of Structures Congress XV*, Portland, USA, April.

Bhuiyan, A.R., Razzaq, M.K., Okui, Y., Mitamura, H. and Imai, T. (2009), "A simplified rheology model of natural and lead rubber bearings for seismic analysis", *Proceedings of the 64th JSCE Annual Conference*,

Fukuoka, Japan, September.

Cao, B.Z., Luo, Q.F., Ma, S. and Liu, J.B. (2002), "Seismic response analysis of Daikai subway station in Hyogoken-Nanbu earthquake", *Earthq. Eng. Eng. Vib.*, **22**(4), 102-107. (in Chinese)

Chopra, A.K. (2007), *Dynamics of Structures: Theory and Applications to Earthquake Engineering*, 3rd Edition, Pearson Prentice Hall, New Jersey, USA.

Das, B.M. (2008), *Advanced Soil Mechanics*, CRC Press, Florida, USA.

Hashash, Y.M.A., Hook, J.J., Schmidt, B. and Yao, J.I.C (2001), "Seismic design and analysis of underground structures", *Tunnel. Underg. Space Tech.*, **16**(4), 247-293.

Hu, J.W. (2015), "Response of seismically isolated steel frame buildings with sustainable lead-rubber bearing (LRB) isolator devices subjected to near-fault (NF) ground motions", *Sustainab.*, **7**(1), 111-137.

Huo, H., Bobet, A., Fernandez, G. and Ramirez, J. (2005), "Load transfer mechanisms between underground structure and surrounding ground: evaluation of the failure of the Daikai Station", *J. Geotech. Geoenviron. Eng.*, **131**(12), 1522-1533.

Hwang, J.S. and Chiou, J.M. (1996), "An equivalent linear model of lead-rubber seismic isolation bearings", *Eng. Struct.*, **18**(7), 528-536.

Iida, H., Hiroto, T., Yoshida, N. and Iwafuji, M. (1996), "Damage to Daikai subway station", *Soil. Found.*, Special Issue, 283-300.

Islam, A.B.M.S., Hussain, R.R., Jumaat, M.Z. and Rahman, M.A. (2013), "Nonlinear dynamically automated excursions for rubber-steel bearing isolation in multi-storey construction", *Auto. Constr.*, **30**, 265-275.

Jangid, R.S. (2007), "Optimum lead-rubber isolation bearings for near-fault motions", *Eng. Struct.*, **29**(10), 2503-2513.

Jangid, R.S. (2010), "Stochastic response of building frames isolated by lead-rubber bearings", *Struct. Control Health Monit.*, **17**(1), 1-22.

JGS-4001-2004 (2006), *Principles for Foundation Designs Grounded on a Performance-based Design Concept*, Japan.

Kelly, T.E., Robinson, W.H. and Skinner, R.I. (2006), *Seismic Isolation for Designers and Structural Engineers*, Robinson Seismic Ltd, Wellington, New Zealand.

Li, Y., Li, Z.L. and Xu, J. (2013), "Study on optimization of bearing parameters for large-scale LRB-based isolated storage tank", *World Earthq. Eng.*, **29**(1), 131-138. (in Chinese)

Matsagar, V.A. and Jangid, R.S. (2004), "Influence of isolator characteristics on the response of base-isolated structures", *Eng. Struct.*, **26**(12), 1735-1749.

Mkrtychev, O.V., Dzhinchvelashvili, G.A. and Bunov, A.A. (2014), "Study of lead rubber bearings operation with varying height buildings at earthquake", *Procedia Eng.*, **91**, 48-53.

Naeim, F. and Kelly, J.M. (1999), *Design of Seismic Isolated Structures: from Theory to Practice*, John Wiley and Sons, New York, NY, USA.

Nagarajaiah, S. and Sun, X.H. (2000), "Response of base-isolated USC hospital building in Northridge earthquake", *J. Struct. Eng.*, **126**(10), 1177-1186.

Park, J.G. and Otsuka, H. (1999), "Optimal yield level of bilinear seismic isolation devices", *Earthq. Eng. Struct. Dyn.*, **28**(9), 941-955.

Parra-Montesinos, G.J., Bobet, A. and Ramirez, J.A. (2006), "Evaluation of soil-structure interaction and structural collapse in Daikai subway station during Kobe earthquake", *ACI Struct. J.*, **103**(1), 113-122.

Providakis, C.P. (2008), "Effect of LRB isolators and supplemental viscous dampers on seismic isolated buildings under near-fault excitations", *Eng. Struct.*, **30**(5), 1187-1198.

Ryan, K.L., Kelly, J.M. and Chopra, A.K. (2005), "Nonlinear model for lead-rubber bearings including axial-load effects", *J. Eng. Mech.*, **131**(12), 1270-1278.

Soong, T.T. and Spencer, B.F. (2002), "Supplemental energy dissipation: state-of-the-art and state-of-the-practice", *Eng. Struct.*, **24**(3), 243-259.

Yamato, T., Umehara, T., Aoki, H., Nakamura, S., Ezaki, J. and Suetomi, I. (1996), "Damage to Daikai subway station of Kobe rapid transit system and estimation of its reason during the 1995 Hyogoken-Nanbu earthquake", *Proceedings of JSCE*, **537**, 303-320. (in Japanese)

Zordan, T., Liu, T., Briseghella, B. and Zhang, Q.L. (2014), "Improved equivalent viscous damping model for base-isolated structures with lead rubber bearing", *Eng. Struct.*, **75**, 340-352.

CC